A&A 410, 685–689 (2003)
DOI: 10.1051/0004-6361:20031352


Astronomy & Astrophysics

*Research Note*

# Differential rotation on UZ Librae

K. Oláh[1], J. Jurcsik[1], and K. G. Strassmeier[2]

[1] Konkoly Observatory of the Hungarian Academy of Sciences, 1525 Budapest, Hungary
e-mail: jurcsik@konkoly.hu
[2] Astrophysical Institute Potsdam (AIP), An der Sternwarte 16, 14482 Potsdam, Germany
e-mail: Kstrassmeier@aip.de

Received 24 April 2003 / Accepted 21 August 2003

**Abstract.** We analysed a time series of nine consecutive years of high-precision photometry of the spotted RS CVn star UZ Lib by using a discrete Fourier-transform technique and a non-linear least-squares minimization. The main period of 4.77 days due to stellar rotation was resolved into three individual periods separated by −0.2% and +0.4% around the main period. The stability of the spot pattern over many years, as derived from our contemporaneous Doppler images, allowed us to relate the different periods to co-existing spots at different latitudes, and thus to the direct determination of the strength and the sign of the differential rotation. The main period originates from the equatorial surface regions and is practically the same as the orbital period from independent radial-velocity measurements, suggesting that the stellar equator is tidally locked to the orbital motion. The higher latitudes rotate slightly faster than the equator, suggesting non-solar differential rotation with a parameter of $\alpha = \Delta\Omega/\Omega = -0.0026$, 80 times weaker than on the solar surface, and a lap time of $P_{\rm equator}/\alpha \approx -1800$ days, i.e. 14 times longer than for the Sun.

**Key words.** starspots – stars: activity – stars: atmospheres – stars: late-type – stars: individual: UZ Lib – stars: binaries: close

## 1. Introduction

Detecting and measuring stellar surface differential rotation is a key project in understanding magnetic activity of late-type stars. The magnitude and sign of the differential rotation pattern puts tight constraints on the possible large-scale magnetic configurations of stars with convective envelopes (e.g. Moss & Tuominen 1997; Kitchatinov & Rüdiger 1999) and will eventually tell us something about the underlying dynamo process (for a summary see Brandenburg & Dobler 2002). However, measuring differential rotation is not without ambiguity and only the first two of the four commonly used methods (correlation of successive Doppler images, direct starspot tracking, Fourier transform of spectral line profiles, Fourier analysis of photometric data) allows the direct extraction of the sign of the differential rotation. In the present paper, we combine two of the four methods (correlation of successive Doppler images, Fourier analysis of photometric data) for application to the spotted K2-giant UZ Librae.

Several attempts have been made to find differential rotation from broad and narrow band photometry, and we give just two examples. Using 15 years of continuous *V*-band data of HR 7275, Strassmeier et al. (1994) found a spot migration rate consistent with a solar-type differential rotation that was only 5–8 times weaker than that on the Sun. Donahue et al. (1996) analysed an about 10 year long dataset of Ca II fluxes of about 100 stars of which 36 stars showed definite signs of multiple periods in their periodograms that the authors associated with surface differential rotation.

Cross-correlation of consecutive Doppler images of spotted stars allows to determine the period shift per latitude bin if there is a suitable tracer, i.e. a cool spot or hot plage, whose lifetime is longer than the time span between the consecutive Doppler images. In this way it is possible to also detect the sign of the differential-rotation parameter $\alpha \equiv \Delta\Omega/\Omega$, where $\alpha > 0$ means the equator rotates faster than the pole, and vice versa for $\alpha < 0$. Donati & Collier Cameron (1997) and Barnes & Collier Cameron (2001) applied this technique to the ultra-rapidly-rotating ZAMS stars AB Dor and PZ Tel and found solar-like differential rotation, i.e. $\alpha > 0$, of comparable strength in terms of $\Delta\Omega$ but approximately a factor of 100 weaker in terms of $\alpha$. Subsequent applications of the Doppler-imaging technique revealed both solar type and non-solar type differential rotation on active stars of various evolutionary states, binary and single (see Weber & Strassmeier 2001 for a more comprehensive summary). From the applications in their series of Doppler images of active stars, Weber & Strassmeier (2001) conclude that the differential rotation pattern on evolved active stars seems to be more complicated

*Send offprint requests to*: K. Oláh, e-mail: olah@konkoly.hu

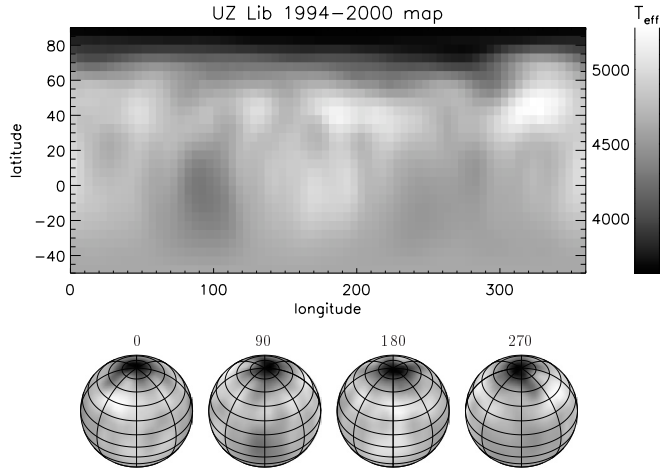


**Fig. 1.** The average Doppler image of UZ Lib for 1994–2000 in pseudo-mercator projection (top). The map is the average of eight maps from seven years (Oláh et al. 2002a). Note the existence of permanent features on the equator and at high latitudes. The spherical projections (bottom) show the stellar surface at longitudes of 0° 90° 180° and 270° according to the orbital ephemeris where 90° and 270° represent the times of conjunctions. Orbital inclination is 50°.

than on active dwarfs, showing a mixture of solar and anti-solar patterns with different strengths. A recent application of the Fourier-transform method to high-resolution spectral line profiles of 142, comparably inactive, field F- and G-stars by Reiners & Schmitt (2003) revealed 10 significant detections of solar-like differential rotation in the range $\alpha/\sqrt{\sin i} = 0.1$–$0.4$ (the inclination, $i$, of the stellar rotational axis remains an unknown in this technique). Thus, all of them are comparable or likely much stronger than the value for the Sun ($\alpha_\odot \approx 0.2$).

Recently, we constructed eight Doppler images of the rapidly-rotating RS CVn binary UZ Librae and used them for a cross-correlation analysis (Oláh et al. 2002a). The surface maps from seven years of time-series spectroscopy is displayed in Fig. 1, averaged and plotted on a single map. Throughout the years a cool polar spot, two appendages of the polar spot at about 60° latitude, and two major equatorial spots co-existed on the surface, the two latter facing the (unseen) companion star and opposite to it. From that, we did not find a coherent signature of differential rotation for latitudes up to 50° from the equator while, on the contrary, the polar-spot appendages above 50° latitude seemed to show a weak acceleration. Because of the overall weakness of the signal ($\alpha \approx 10^{-3}$), we were not able to unambiguously conclude the existence of true non-solar differential rotation on UZ Librae. However, our two studies (Oláh et al. 2002a,b) verified that UZ Lib exhibits a stable spot configuration over the course of several years, which is a mandatory physical requirement if we want to detect differential rotation in the Fourier spectrum of a ground-based, years-long photometric dataset with all its basic shortcomings of (very) uneven sampling. Consequently, UZ Lib represents a possible candidate to identify differential rotation in the Fourier spectrum. In this paper we use the ≈1700 photometric data points obtained with automatic photoelectric telescopes between 1993 and 2001. Section 2 briefly describes our Fourier technique, Sect. 3 presents the results from the application to the UZ Librae photometry, and Sect. 4 discusses the results.

## 2. Data, method and numerical simulations

Nine years of continuous Johnson-Cousins *VI*-band photometry from the Amadeus 0.75 m automatic photoelectric telescope (APT) at the Fairborn Observatory in Arizona is used in this paper. Its overall data quality is near 5 mmag in *V* over the course of its operation (for details of the data see Oláh et al. 2002b); this *V* dataset was used in the present paper.

We apply the program package MUFRAN (that uses standard Fourier and least-squares minimalization techniques, Kolláth 1990) which was developed for studying multi-periodic unevenly-sampled data. Our analysis strategy incorporates three consecutive steps. First we follow the succesive steps of calculating Discrete Fourier Transforms (DFT) and prewhitening the data with the detected frequency components. Then, we search for the best-fit frequency combinations with the help of non-linear least-squares method. Finally, the reality of the best solution is verified by checking the existence of the three frequency components found from the whole dataset in three-year long subsets.

The presence of the long-term cyclic variability of UZ Lib (Oláh et al. 2002b) has practically no effect in the rotational regime of the Fourier spectrum. We find that using the dataset pre-whitened with the short frequencies or just as observed give the same results well within the errors. Therefore the long-term trend remained in the data. A more detailed description dealing with long-term changes and comparison with other methods was given in Oláh et al. (2000).

A feasibility study for the detection of differential rotation from long and uninterrupted photometry was recently presented by Strassmeier & Oláh (2003) for the ESA space mission *Eddington* (Favata 2001). In these simulations, we used the results of the spot modelling of UZ Lib from Oláh et al. (2002b) as a starting point. A spherical stellar model was prepared based on the actual stellar parameters of UZ Lib and included spots at the positions derived from the modelling of the original data. We then applied differential rotation to the stellar surface and generated a large number of artificial light curves. These light curves were then subjected to the same type of analysis as presented in this paper and had shown that discrete rotational periods can be extracted from up to five latitudinal bins.

## 3. Results

The Fourier spectrum of the APT photometry is plotted in the upper panel of Fig. 2. The UZ Lib spectrum shows a complex structure around the value of the rotational frequency (that should be close to the orbital frequency of the binary which is 0.20972 cycle/day, Fekel et al. 1999), probably due to multiple periodicities, and a much more simple pattern in the harmonic regime corresponding mainly to one frequency component. The details of the spectral features around 0.21 cycle/day and in the first harmonic regime (around 0.42 cycle/day) are enlarged in the inserts. For comparison, the spectral window is shown in the bottom panel of Fig. 2. The noise level of

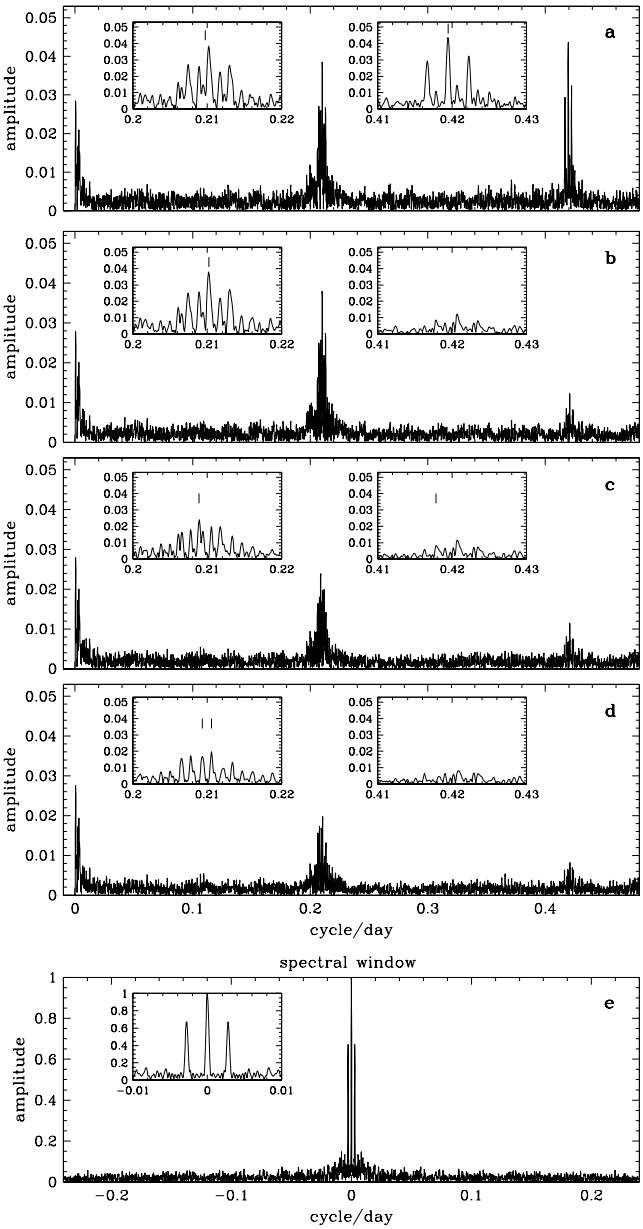


**Fig. 2. a)** Amplitude spectrum of all photometric data from 1993−2001. The inserts show details of the spectra around 0.21 cycle/day (in the vicinity of the rotation frequency of the star) and of the first harmonic regime around 0.42 cycle/day. Due to the double-humped light curve of UZ Lib the frequency with the largest amplitude is around 0.42 cycle/day, this, and the corresponding main frequency are marked in the right and left inserts, respectively. **b)** Amplitude spectrum after the first main frequency and its harmonic have been removed. In the left insert the highest amplitude frequency around 0.21 cycle/day is marked. **c)** Amplitude spectrum after the second frequency was removed. A significant amplitude around the main frequency and its first harmonic with small amplitude have remained. **d)** Amplitude spectrum after the removal of the third dominant frequency and its harmonic. Note that frequencies of up to $0\overset{\mathrm{m}}{.}02$ in amplitude still remained near the main frequency suggesting a very complex rotational surface pattern. For comparison, panel **e)** shows the spectral window and its structure around 0 cycle/day.

the spectra shown in Figs. 2a–c is about 0.003 mag, therefore signals larger than 0.009 mag are supposed to be real. Concerning the harmonic components a less conservative $2\sigma$ criterion is applied, namely all harmonic components with amplitude larger than 0.006 mag are taken into account in the solutions. No second harmonic component of any of the three frequencies exceeds this amplitude limit in the final solution when fitting the data simultanously with the three components and their harmonics.

The highest amplitude in the Fourier spectrum is at 0.41944 cycle/day which is in fact the first harmonic ($2f_1$) of the most prominent rotational feature ($f_1$) with a double-humped shape. After the removal of this signal from the data the next two consequent spectra (Figs. 2b–c) reveal two further frequency components in the vicinity of the rotational frequency ($f_2 = 0.21017$ and $f_3 = 0.20890$ cycle/day); $2f_3$ can also be detected with a small but real amplitude. These frequencies are marked in the inserts of the original and the successively pre-whitened spectra in Fig. 2. The residual spectrum in Fig. 2d still shows signals of $\approx 0\overset{\mathrm{m}}{.}02$ at 0.21056 and 0.20932 cycle/day. We interpret these residual frequencies in the next section.

As the amplitudes of the three components are not indeed significantly different, prewhitening with the frequencies in different sequences and fitting the data with two and/or three components simultaneously by nonlinear least squares method were also checked. As a result, all the solutions led to the detection of the three frequency components listed above. To refine the frequencies and to estimate the amplitudes of the components and their harmonics a three-frequency nonlinear least square fit to the data was calculated with the result given in the first line in Table 1.

The most likely explanation of these three, closely-spaced frequencies is differential surface rotation. The contemporaneous Doppler images support this interpretation because it showed long-lived surface features at different latitudes of the star. We cannot exclude the principle possibility that these three frequencies actually correspond to a single signal with a period that is varying in time. However, it would require that its "variability" remained stable for long enough intervals in time in order to appear as distinct frequencies in the power spectrum. Such a scenario could be produced e.g. by a single spot changing its latitude from time to time. In order to check and/or exclude this possibility, we splitted the nine-year long dataset into three parts, each of them three years long, and analysed these subsets separately. If the three detected frequencies found in the nine-year long dataset can be also detected in the subsets it would strongly indicate that these periodicities can be indeed identified with the simultaneous existence of differentally rotating surface configurations.

Figure 3 summarizes the analysis of the three independent data subsets, each of them three years long. Unfortunately, searching for closely-spaced periodicities in these limited datasets cannot lead to unique solutions. This is easily seen in Fig. 3d where the width of the frequency peaks is now about three times larger than in the spectra from the full dataset, and becomes of the same order of the frequency separation itself ($\approx$0.0006 cycle/day). The 3-year long dataset is simply not sufficient for the direct detection of such close frequencies (and thus differential rotation).

**Table 1.** Results from the period search of the whole dataset and its subsets (# 1, # 2, # 3). $P$ is the period, $f$ the frequency, and $A$ the semiamplitude in $V$. The errors in frequency/period come from the widths of the spectral lines and are practically the same for all components in one dataset. The lower row connects the detected periodicities with the surface features from the contemporaneous Doppler images.

| Data set | $P_1$ [days] | $f_1$ [cycle/day] | $A(f_1)$ [mag] | $A(2f_1)$ | $P_2$ [days] | $f_2$ [cycle/day] | $A(f_2)$ [mag] | $A(2f_2)$ | $P_3$ [days] | $f_3$ [cycle/day] | $A(f_3)$ [mag] | $A(2f_3)$ |
|---|---|---|---|---|---|---|---|---|---|---|---|---|
| all | 4.7683(07) | 0.20972(03) | 0.008 | 0.044 | 4.7581 | 0.21017 | 0.037 | … | 4.7870 | 0.20890 | 0.025 | 0.009 |
| # 1 | 4.7694(36) | 0.20967(16) | 0.017 | 0.035 | 4.7567 | 0.21023 | 0.064 | 0.006 | 4.7751 | 0.20942 | 0.067 | … |
| # 2 | 4.7687(25) | 0.20970(11) | 0.017 | 0.048 | 4.7495 | 0.21055 | 0.025 | 0.016 | … | … | … | … |
| # 3 | 4.7663(16) | 0.20985(07) | 0.038 | 0.048 | 4.7515 | 0.21046 | 0.010 | 0.007 | 4.7849 | 0.20899 | 0.030 | … |
| | equatorial spots | | | | polar-spot appendages | | | | short-lived features | | | |

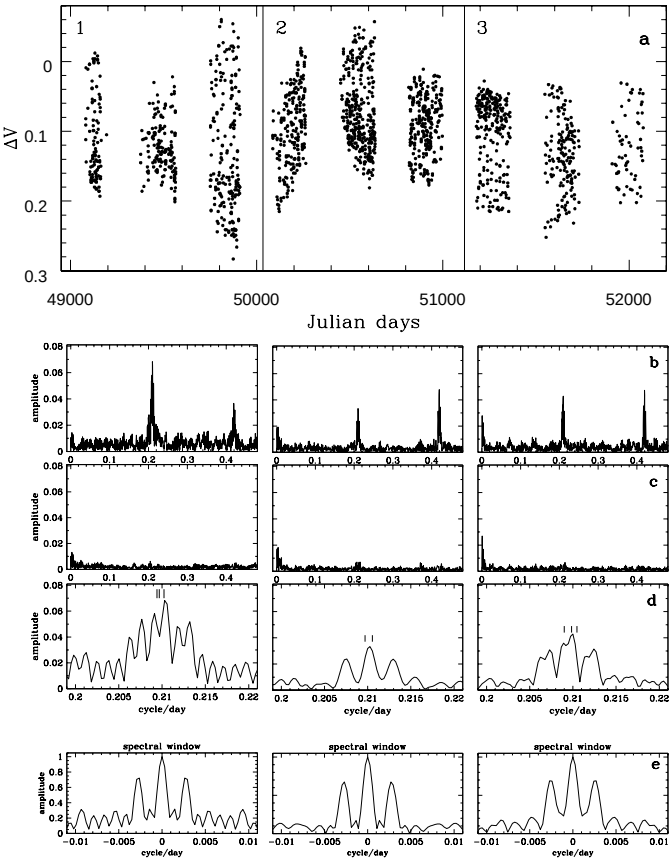


**Fig. 3.** Results from the analysis of three data subsets. **a)** Full data between 1993–2001 divided into three parts (Cols. 1–3), each subset is 3-year long. **b)** Fourier-amplitude spectra of the three datasets. **c)** The spectra after removal of the frequencies $f_1$–$f_3$ and their harmonics listed in Table 1. None of the residual spectra shows signals larger than $0\overset{m}{.}006$ near the rotational frequency. Note that the peak at very low frequencies is due to the long term variation of the data, evident in the top panel. **d)** Details of the spectra close to the rotational frequency, with the resulting frequencies marked. The separation of the detected periods are similar or even smaller than the widths of the individual lines which makes successive identification of the real components impossible. **e)** A close-up of the corresponding spectral windows.

We can nevertheless check the subsets for the presence of the three frequencies that were found in the whole dataset by evaluating their least-squares solutions under the assumption that these frequencies are indeed in the data. To determine the actual values of the periods and amplitudes three-component non-linear least-squares fits to the subsets were performed. If there was any indication that the first harmonic of a frequency also showed up in the spectra this was taken into account. Solutions with frequencies close to the original values and with reasonable amplitudes were obtained which validates that the frequency components listed in the first line of Table 1 are indeed present in the subsets. The respective least-squares solutions converged on consistent frequencies and reliable amplitudes, which are shown in Fig. 3 and summarized in Table 1. It is important to note that the solutions of the subsets obtained from the a priori assumption of the existence of these frequencies were always more accurate (resulted in smaller residual ampitudes) than any straightforward 3-frequency direct fit to the subsets.

Table 1 lists the periods $P_i$ and frequencies $f_i$ ($i = 1, 2, 3$ stands for the three frequencies detected) and their respective amplitudes $A(f_i)$ for both the full dataset and the three subsets. (We note that in this paper Fourier-amplitudes are given which correspond to the semiamplitudes of the real variations.) The amplitudes of the harmonics, if detected, are also indicated. The errors of the periods were estimated by increasing the residual scatter of the least-squares solutions by $0\overset{m}{.}0005$ which corresponds to 10% of the precision of the data used (cf. Press et al. 1992).

## 4. Discussion and conclusions

Our analysis of nine years of data of UZ Lib revealed three close periods around the expected rotational period of 4.768 days, that is close to the orbital period. Based on the repeatability of this result from subsets of the full data, we conclude that two of them ($P_1$ and $P_2$) can be related to long-lived features seen in our averaged Doppler image, while the third period ($P_3$ in Table 1) most likely stems from shorter living features.

The single determinations of the values of $P_1$ in each of the subsets agree within the $3\sigma$ error limits. The same is seen for $P_2$. However, there is a slight indication that $P_1$ is slightly decreasing by ≈0.1% during the nine years of observations, possibly indicating a dependency on the activity cycle. From Table 1 it is seen that the first harmonic of $P_1$ always has a larger amplitude than $P_1$ itself. Actually, this harmonic

frequency has the highest amplitude in the spectra and its real component around the rotational frequency appears comparably weak. We identify this main frequency and its harmonic with the rotational modulation due to the two permanently spotted regions on the stellar equator 180° apart, as depicted from Fig. 1. Such a spot configuration results in a double-humped light curve with two minima separated by half the rotational period (see Oláh et al. 2002b) and explains the high power at the harmonic component. Thus we conclude, that $P_1$ is the true rotation period of the star at the equator. The second and shortest of the three periods ($P_2$) can be related to the polar-spot appendages and interpreted as the rotational period at that latitude (60–65°). Its first harmonic is also present in the subsets, though with smaller amplitude. The third period ($P_3$) is possibly due to shorter living features that either have proper motions in addition to the rotation or just mimic a periodic signal because of a variety of different growth and decay times.

According to the data listed in Table 1 it can be also seen that the two frequencies appearing in the residual spectrum of the full dataset with about $0\overset{\mathrm{m}}{.}02$ amplitude (Fig 2d, 0.21056 and 0.20932 cycle/day), can be identified with the frequencies $f_2$ in subset 2. and $f_3$ in subset 1., respectively. These frequencies seem to be simply shifted a little from the values of $f_2$ and $f_3$ resulting from the whole dataset, thus cannot be regarded as independent additional signals.

The orbital period of $4\overset{\mathrm{d}}{.}76824 \pm 0.000026$ (Fekel et al. 1999) is well within the respective $1\sigma$ error bars of our rotational period on the equator, i.e. $4\overset{\mathrm{d}}{.}7683 \pm 0.0007$. This strongly suggests that the equatorial regions of UZ Librae are tidally locked to the orbital motion. Simple dynamo models for close (but detached) binary systems put forward by Moss & Tuominen (1997) result in large-scale non-axisymmetric magnetic surface fields having maxima at the intersection of the apsidal line with the stellar surfaces, with field lines symmetric with respect to the orbital plane, and thus in agreement with our observations.

The period at high latitudes, $4\overset{\mathrm{d}}{.}7581 \pm 0.0007$ for latitudes of around 60–65°, differs by 15-$\sigma$ from the equatorial value. If we assign $\beta = 65°$ as the average latitude of the polar appendages, we find from $P_\beta/P_{\mathrm{equ}} = 1 - \alpha \sin^2\beta$ the differential-rotation parameter $\alpha = -0.0026$, i.e. a small but significant anti-solar differential rotation pattern, as was already suggested from the cross-correlation of individual Doppler maps by Oláh et al. (2002a). The corresponding lap time, $2\pi/\Delta\Omega$ or $P/\alpha$, i.e. the time the equatorial spots need to lap the polar-spot appendages, is ≈1800 days. This is the first *direct* detection of differential rotation of an active star from Fourier analysis of its long-term broad-band photometric data. We would like to emphasize that it was the long-term stability of the surface pattern of UZ Lib that enabled this detection.

*Acknowledgements.* We appreciate the remarks of the referee Dr. P. Amado that helped us to significantly improve the paper. KO and JJ acknowledge financial support from the Hungarian government through OTKA T-030954, T-032846, T-038013, T-043504, and from the Hungarian-German Intergovernmental grant D21/01. KGS acknowledges support from the German Science Foundation (DFG) grant STR645/1.

## References

Barnes, J. R., & Collier Cameron, A. 2001, MNRAS, 326, 950
Brandenburg, A., & Dobler, W. 2002, AN, 323, 411
Donahue, R. A., Saar, S. H., & Baliunas, S. L. 1996, ApJ, 466, 384
Donati, J.-F., & Collier Cameron, A. 1997, MNRAS, 291, 1
Favata, F., Roxburgh, I., & Galadi, D. (eds.) 2001, 1st Eddington Workshop, ESA SP-485
Fekel, F. C., Strassmeier, K. G., Weber, M., & Washuettl, A. 1999, A&AS, 137, 369
Kitchatinov, L. L., & Rüdiger, G. 1999, A&A, 344, 911
Kolláth, Z. 1990, The program package MUFRAN, Occ. Techn. Notes of Konkoly Obs., No. 1 (www.konkoly.hu/Mitteilungen/Mitteilungen.html)
Moss, D., & Tuominen, I. 1997, A&A, 321, 151
Oláh, K., Kolláth, Z., & Strassmeier, K. G. 2000, A&A, 356, 643
Oláh, K., Strassmeier, K. G., & Weber, M. 2002a, A&A, 389, 202
Oláh, K., Strassmeier, K. G., & Granzer, T. 2002b, AN, 323, 453
Press, W. H., Teukolsky, S. A., Vetterling, W. T., & Flannery, B. P. 1992, Numerical Recepies in FORTRAN: The Art of Scientific Computing, 2nd ed. (New York: Cambridge Univ. press)
Reiners, A., & Schmitt, J. H. M. M. 2003, A&A, 398, 647
Strassmeier, K. G., Hall, D. S., & Henry, G. W. 1994, A&A, 282, 535
Strassmeier, K. G., & Oláh, K. 2003, in Second Eddington Workshop, ed. F. Favata, Palermo, ESA SP, in press
Weber, M., & Strassmeier, K. G. 2001, A&A, 373, 974